Proc. Natl. Acad. Sci. USA
Vol. 79, pp. 1854–1858, March 1982
Biophysics

Oxygen transport parameter in membranes as deduced by saturation recovery measurements of spin-lattice relaxation times of spin labels

(pulse ESR/diffusion and concentration of oxygen/phase transitions)

AKIHIRO KUSUMI, WITOLD K. SUBCZYNSKI*, AND JAMES S. HYDE†

National Biomedical ESR Center, Department of Radiology, The Medical College of Wisconsin, Milwaukee, Wisconsin 53226

Communicated by George Feher, December 7, 1981

ABSTRACT **Spin-lattice relaxation time (T_1) measurements of nitroxide radical spin labels in membranes have been made by using the saturation-recovery technique. Stearic acid and sterol-type labels were used as probes of dimyristoylphosphatidylcholine liposomes from 0°C to 36°C. In the absence of oxygen, the range of variation of T_1 over all samples and conditions is about a factor of 3. Heisenberg exchange between oxygen and spin labels is an effective T_1 mechanism for the spin labels. The full range of variation of T_1 in the presence of air is about a factor of 100. It is suggested that the oxygen transport parameter $W = T_1^{-1}$ (air) − T_1^{-1} (N_2) is a useful new monitor of membrane fluidity that reports on translational diffusion of small molecules. The values of W change at the prephase and main phase transitions and vary in complex ways. Arguments are advanced that the data are indicative of anisotropic translational diffusion of oxygen.**

Nitroxide radical spin labels have been used extensively to probe the dynamic structure of synthetic and biological membranes (1). Increasingly, so-called nonlinear ESR methods have been applied to membranes including saturation transfer spectroscopy (see ref. 2 for a review with emphasis on membranes), electron-electron double resonance (ELDOR) (3), and continuous-wave (CW) saturation (4). In these nonlinear methods, the basic "clock" that establishes the time scales over which dynamic information can be obtained is the electron spin-lattice relaxation time T_1. The rationale of the nonlinear methods is that T_1 is relatively long, (1–10 μsec), permitting the investigation of slower processes than is possible by using linear methods.

There is reasonable evidence that T_1 of spin labels varies relatively little over a wide range of conditions. It would be a disadvantage in use of nonlinear methods if T_1 were extremely sensitive in itself to the motions under investigation. However, no measurement of T_1 has ever been reported for a spin-label in a membrane, and only one measurement exists for a spin-label in aqueous media—that of Huisjen and Hyde (5) for maleimide-labeled hemoglobin. The experimental difficulty lies in the high dielectric loss of water and the fact that pulse measurements on a time scale of microseconds are technically difficult. Nonlinear spin-label methods cannot progress further without knowledge of T_1s and that is a principal object of the present work.

We have developed a high-speed data receiver-processor (6) for enhancement of the signal-to-noise ratio in time domain ESR. Because the intrinsic ESR signal-to-noise ratio of spin-labeled membranes is small, extensive signal averaging is required in pulse ESR. Because T_1 is of the order of microseconds, the overall repetition rate of the experiment can be as high as able time. Fast analog-to-digital conversion and fast adding of the acquired signals is required. This has been accomplished. Data presented here typically represent $>10^7$ accumulations obtained in several minutes.

Popp and Hyde (3) observed that nonlinear ESR experiments in membranes are seriously and adversely affected by the presence of molecular oxygen. They introduced a convenient means for removing O_2 from membrane samples based on sample tubes fabricated from a gas-permeable plastic known as TPX.

From analysis of CW saturation data, Subczynski and Hyde (4) argued that Heisenberg exchange between oxygen and spin labels is an effective T_1 mechanism for the spin labels. The present work confirms this effect directly. They observed discontinuities in CW saturation characteristics of air-saturated membranes, and these discontinuities substantially disappeared in the absence of oxygen.

Heisenberg exchange is governed by the bimolecular collision rate which depends on concentration and on diffusion. Both can be expected to change.

Now that it has become possible to observe T_1s directly, we have reexamined the effects of O_2 on spin-label T_1s in membranes. The effects are remarkable, with total variation, over all conditions, of about a factor of 100.

We define an oxygen transport parameter

$$W = T_1^{-1}\,(\text{air}) - T_1^{-1}\,(N_2),$$

which is a function of both concentration and translational diffusion of oxygen in the membrane. We have compared this parameter with conventional spin-label fluidity parameters that depend on rotational diffusion of the labels rather than on translational diffusion of a small molecule, O_2. Both displays reflect the phase transitions, but there are few other similarities. It appears that the W is a useful indication of membrane viscosity as it is experienced by small molecules.

There are competing methods for observing oxygen effects in membranes—quenching of pyrene fluorescence by oxygen (7), proton NMR (8), and ESR spin-label line-broadening (9).

MATERIALS AND METHODS

Spin labels were obtained from Syva (Palo Alto, CA) and L-α-dimyristoylphosphatidylcholine (Myr_2PtdCho) from Sigma.

The publication costs of this article were defrayed in part by page charge payment. This article must therefore be hereby marked "*advertisement*" in accordance with 18 U. S. C. §1734 solely to indicate this fact.

Abbreviations: T_1, spin-lattice relaxation time; CW, continuous wave; Myr_2PtdCho, L-α-dimyristoyl-phosphatidylcholine; ASL, androstane spin label; CSL, cholestane spin label; 5-SASL, 5-doxylstearic acid spin label; 16-SASL, 16-doxylstearic acid spin label. Structures of spin labels are shown in Fig. 1.

* On leave from The Department of Biophysics, Institute of Molecular Biology, Jagiellonian University, Krakow, Poland.
† To whom reprint requests should be addressed.

$Myr_2PtdCho$ and spin label were mixed in chloroform and then dried with a stream of nitrogen gas. Molar ratios of spin label to $Myr_2PtdCho$ were 1:100 for androstane spin label (ASL), cholestane spin label (CSL), and 5-doxylstearic acid spin label (5-SASL), and 1:200 for 16-doxylstearic acid spin label (16-SASL). Residual lipids were further dried under reduced pressure (≈0.1 mm Hg) for at least 12 hr. Liposomes (multilamellar dispersion of lipids) were formed by adding buffer solutions (200 mM Hepes at pH 7.7 for the experiments with ASL and CSL; 100 mM sodium borate at pH 9.5 for the experiments with 5-SASL and 16-SASL) to dried lipid at 35°C and shaking by hand in the water bath at 35°C. Liposomes were centrifuged at 12,800 × *g* for 10 min at 4°C, and the loose pellet was used for ESR measurements.

Samples were placed in a gas-permeable capillary (inner diameter, 0.8 mm) made from the methylpentene polymer TPX (3, 4). This plastic is permeable to oxygen, nitrogen, and carbon dioxide and is substantially impermeable to water. The concentration of oxygen in the sample was controlled by equilibrating the sample with the same gas that was used for temperature control, a mixture of nitrogen and dry air. The flows of nitrogen and air were measured and adjusted by flowmeters (Matheson Gas Products, 7630 series) to obtain desired ratios of mixtures.

Spin-lattice relaxation times were measured at X-band by using the saturation-recovery technique. An intense and long-duration saturating pulse tends to equalize the populations. The return to equilibrium is then monitored with a weak observing power. The method has been reviewed by Hyde (10).

The apparatus used here was based in part on the design of Huisjen and Hyde (5) and Percival and Hyde (11). The three-arm microwave bridge is essentially identical, although a 10-W TWT amplifier (Logimetrics A200/X) was introduced to increase the pumping power, and pump-arm phase modification is now accomplished by a pin-diode phase shifter (Triangle MP-72). These early instruments used a single channel boxcar; the present receiver (6) has an adjustable number of apertures for each recovery signal from 16 to 512. A new type of bimodal microwave cavity has been designed: two crossed cylindrical TE_{112} modes with the axis of the cavity parallel to the magnetic field. All data were obtained with 50-Hz pump-phase modulation for suppression of free-induction decay signals and 25-Hz field modulation for improvement of overall spectrometer stability. Data were obtained in the tails of recovery curves to minimize errors from pseudosecular contributions to the signal (5, 10–13). Typical overall repetition rates were between 20 and 50 kHz, accumulating 2×10^7 additions.

More details of the bimodal cavity and the data receiver-processor will be published elsewhere.

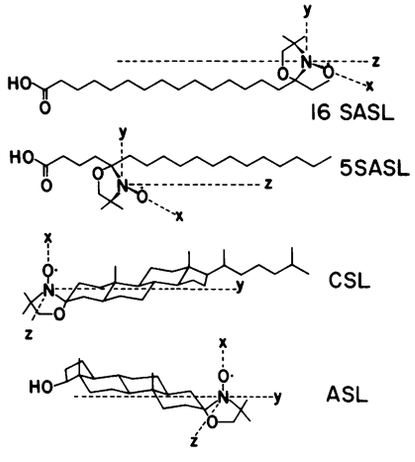

FIG. 1. Structures of spin labels used in this work, showing principal axes. Spin labels are intercalated in the membrane with the hydrophilic part (left-hand side) on the surface of the membrane. The nitroxide moieties of 5-SASL and CSL are close to the surface; those of 16-SASL and ASL are near the middle of the bilayer.

RESULTS AND DISCUSSION

Characterization of the System. Structures of the spin labels used in this work are shown in Fig. 1. The principal molecular

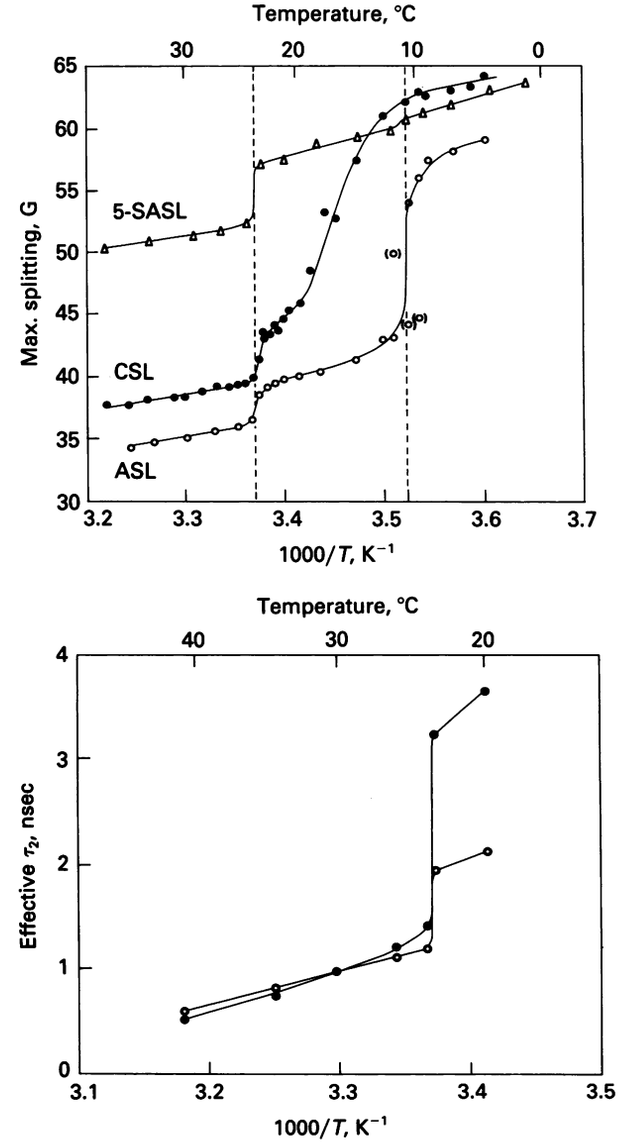

FIG. 2. (*Upper*) Maximal splitting values of 5-SASL (△), ASL (○), and CSL (●) plotted against reciprocal temperature. ASL showed two components around the pretransition temperature. The minor component is shown in parentheses. (*Lower*) Effective rotational correlation time of 16-SASL plotted against reciprocal temperature. ○, Calculated from the linear term of the linewidth parameter, $\tau_{2B} = 6.51 \times 10^{-10}\ \Delta H(0)[(h_0/h_{-1})^{1/2} - (h_0/h_{+1})^{1/2}]$ sec; ●, calculated with the quadratic term, $\tau_{2C} = 6.51 \times 10^{-10}\ \Delta H(0)[(h_0/h_{-1})^{1/2} + (h_0/h_{+1})^{1/2} - 2]$ sec. $\Delta H(0)$ is the peak-to-peak width of the central ($M_I = 0$) line, and h_{+1}, h_0, and h_{-1} are heights of the low ($M_I = +1$), central ($M_I = 0$), and high ($M_I = -1$) field peaks, respectively.

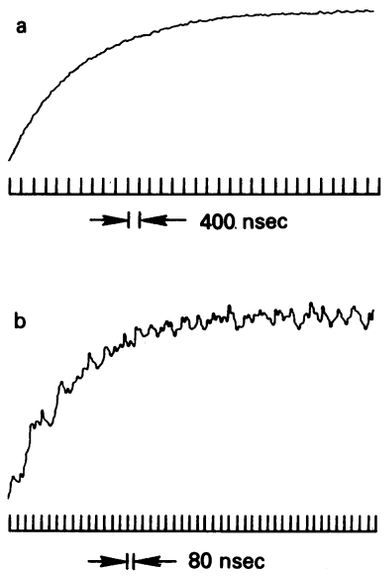

FIG. 3. Typical saturation recovery signals. (*a*) 16-SASL in $Myr_2PtdCho$ at 22.8°C equilibrated with nitrogen. T_1 = 2.46 μsec. Conditions: pump power, 240 mW; pump width, 5 μsec; observing power, 3.0 mW; width of 25-Hz field modulation, 0.5 G; 1.6×10^7 additions. (*b*) 16-SASL in $Myr_2PtdCho$ at 28.2°C equilibrated with 50% air. T_1, 0.56 μsec. Conditions: pump power, 1.2 W; pump width, 0.7 μsec; observing power, 4.8 mW; width of 25-Hz field modulation, 0.8 G; 3.3×10^7 additions. Data were collected for 11 min in both cases.

axes are nearly parallel to the normal of the bilayer above the phase transition temperature of $Myr_2PtdCho$, but a cooperative tilt of ca. 30° has been observed near the surface of the membrane (14, 15) and a tilt angle of ca. 23° has been reported for dipalmitoylphosphatidylcholine below the transition temperature (16). The *x* axis (along the N—O bond) is perpendicular to the long axis of the molecule in every case. The principal p_z axis of the nitroxide is parallel to the molecular long axis for stearic acid spin labels (5-SASL, 16-SASL) and is perpendicular for sterol-type spin labels (ASL, CSL).‡ It is noted that the sterol-type labels are fairly rigid and the spin label reports the motion as a whole, whereas segmental motions of the alkyl chain (*gauche-trans* isomerism) play important roles in determining the ESR spectra of stearic acid spin labels.

The apparent pK of 5-SASL in multilamellar dispersions of egg yolk phosphatidylcholine was reported to be 6.2 (19), but we found evidence, above the phase-transition temperature of $Myr_2PtdCho$, for a mixture of protonated and unprotonated labels at pH as high as 8.0 for 5-SASL and 9.0 for 16-SASL. Therefore, the present experiments were run at the rather high pH of 9.5. In 16-SASL there was still some indication of two components in the spectrum below the phase-transition temperature. The physical properties of phosphatidylcholine membranes have been shown to be insensitive to pH in the range 4.2 to 12 (20, 21). ASL and CSL spin labels exhibit no pH sensitivity between 4.5 and 9.5. Data reported here for these labels were obtained at pH 7.7.

The response of the system to change of temperature is slow below the pretransition temperature. In the present work, samples were equilibrated above the main transition temperature, the temperature was then lowered to the desired value, and the sample was equilibrated for at least 1 hr before data were collected.

Rotational diffusion ESR data for the four spin labels are shown in Fig. 2. Maximal splittings for ASL, CSL, and 5-SASL are plotted in Fig. 2 *Upper*. ASL (label near the center of the bilayer) shows well-defined steps at both the main and pretransitions. CSL (label near the surface) shows effects at the main transition that are similar to those of ASL but the pretransition is not detected. 5-SASL (label near the surface) reflects the main transition but evidence for the pretransition is slight.

‡ For the stearic acid spin labels there may be tilt of ca. 30° in the time scale of 0.1 μsec (15). For sterol-type spin labels this may not be exactly correct. A small deviation has been reported (17). The steroid spin labels exist in two epimeric forms (18). They are unresolvable spectrometrically.

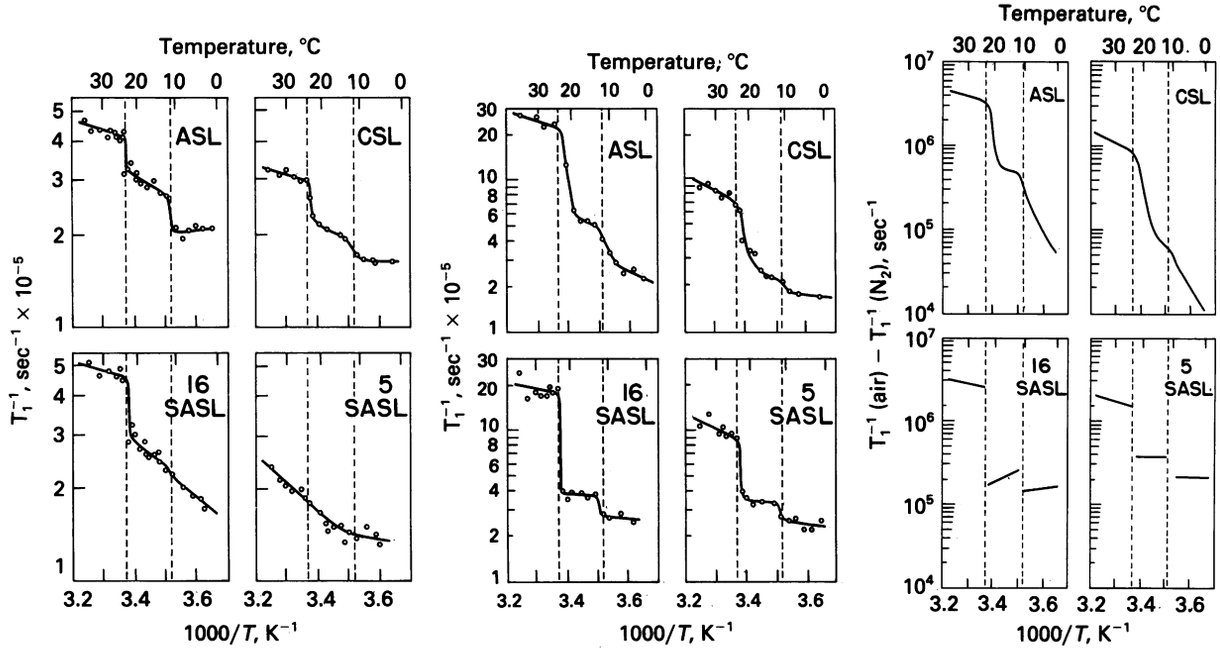

FIG. 4. (*Left*) T_1^{-1} vs. T^{-1} under nitrogen. (*Middle*) T_1^{-1} vs. T^{-1} in the presence of 50% air. (*Right*) Oxygen transport parameter [$W = T_1^{-1}$ (air) − T_1^{-1} (N_2)] vs. T^{-1}.

16-SASL exhibits so much motion that a different display is required (Fig. 2 *Lower*). The effective correlation time, assuming isotropic rotational diffusion, has been calculated by using both the linear and quadratic terms (22). When these two values are similar it is argued that the motional model is fairly good. This is the situation above the main transition temperature. The spectrum of 16-SASL changes abruptly and the linear and quadratic values differ substantially below this temperature, indicating the onset of anisotropic rotational diffusion. 16-SASL is in the slow tumbling regime near the pretransition temperature and no convenient parameterization has been established.

Measurement of T_1 in the Absence of Molecular Oxygen. All measurements of T_1 were made for the central line ($M_I = 0$). Typical saturation-recovery curves are shown in Fig. 3. These curves can serve as an approximate guide to the signal-to-noise ratio that can be expected from a spin-labeled membrane in aqueous media with an average spin-label concentration of 3–4 mM, but the equipment is still being modified and no smoothing or computer-aided filtering of the data has yet been introduced. The data are plotted in Fig. 4 *Left*. Least squares linear fits were made for each of the intervals between the broken lines (which are drawn at the phase transition temperatures) and the straight lines and then connected by eye.

The following points can be made.

a. Abrupt changes in T_1 were observed at the main and pretransition temperatures for ASL, CSL, and 16-SASL but not for 5-SASL. This result suggests that motion of the nitroxide z axis about the x,y axes contributes to the relaxation more than x-y averaging.

b. T_1s for 16-SASL and ASL (label at the center of the bilayer) tend to be shorter than for 5-SASL and CSL (label near the surface).

c. The overall range of variation is about a factor of 3. The range of variation is thought to be sufficiently small and these spin labels sufficiently typical that these values could be used safely in interpretation of nonlinear ESR experiments on membranes.

d. The motional effects (Fig. 2) also depend on motion about x,y axes, and as a general rule Figs. 2 and 4 are similar. However, at the pretransition temperature, CSL in Fig. 2 showed no inflection although it was seen in Fig. 4. Conversely, both transitions were detectable for 5-SASL in Fig. 2 but not in Fig. 4. Thus, the two approaches appear to have a complementary character, although further investigation is required to understand the differences.

e. Subczynski and Hyde (4) observed little discontinuity in $P_{1/2}$ (the incident power at which the ESR signal is half as great as it would have been in the absence of saturation) at the main transition temperature of $Myr_2PtdCho$ with stearic acid spin labels. As they suggested in their report, it is likely that almost equal and opposite changes in T_1 and T_2 at the transition temperature result in a continuity of $P_{1/2}$. This seems also to be the case for sterol-type spin labels (see Fig. 6).

Measurement of T_1 in the Presence of Molecular Oxygen. Fig. 4 *Middle* shows plots of T_1^{-1} as a function of reciprocal temperature for samples equilibrated with 50% air/50% N_2. The straight lines were obtained by a least squares fitting; for the sterol spin labels, a smooth curve was drawn in the region between the phase transitions.

Fig. 5 shows the dependence of T_1^{-1} on the concentration of molecular oxygen (air), which is observed to be linear under all conditions. Based on the likely assumption of Subczynski and Hyde (4) that the interaction between oxygen and spin label is Heisenberg exchange, the contribution to the effective T_1 is governed by the bimolecular collision rates. We obtain

$$T_1^{-1}\,(\text{with } O_2) - T_1^{-1}\,(\text{without } O_2) \propto D_o[O_2],$$

where D_o is the diffusion constant of oxygen and $[O_2]$ is the concentration of oxygen at a given locus.

The large changes in T_1 shown in Fig. 4 *Middle* are due in part to temperature-dependent solubility of oxygen in membranes and in part to the temperature dependence of D_o. The absolute concentration of oxygen in $Myr_2PtdCho$ varies by about a factor of 15 between 5°C and 40°C (unpublished data). Thus, tentatively, the observed effects arise from a significant temperature dependence of both solubility and diffusion.

Subczynski and Hyde (4) have reported $P_{1/2}$ measurements for stearic acid spin labels in the presence of oxygen. Fig. 6 shows similar data for the sterol spin labels. In general the intrinsic T_2s of the spin labels are so short in the absence of oxygen that the additional contribution of oxygen is insignificant. The main effect of oxygen on $P_{1/2}$ comes from the change of T_1 (effective). The distinction between T_1 and T_1 (effective) leads to a complication in relating $P_{1/2}$ to T_1 data (see equation 7 in ref. 4). Motionally induced nitrogen nuclear relaxation generally contributes a factor of 3 to the effective spin-lattice relaxation

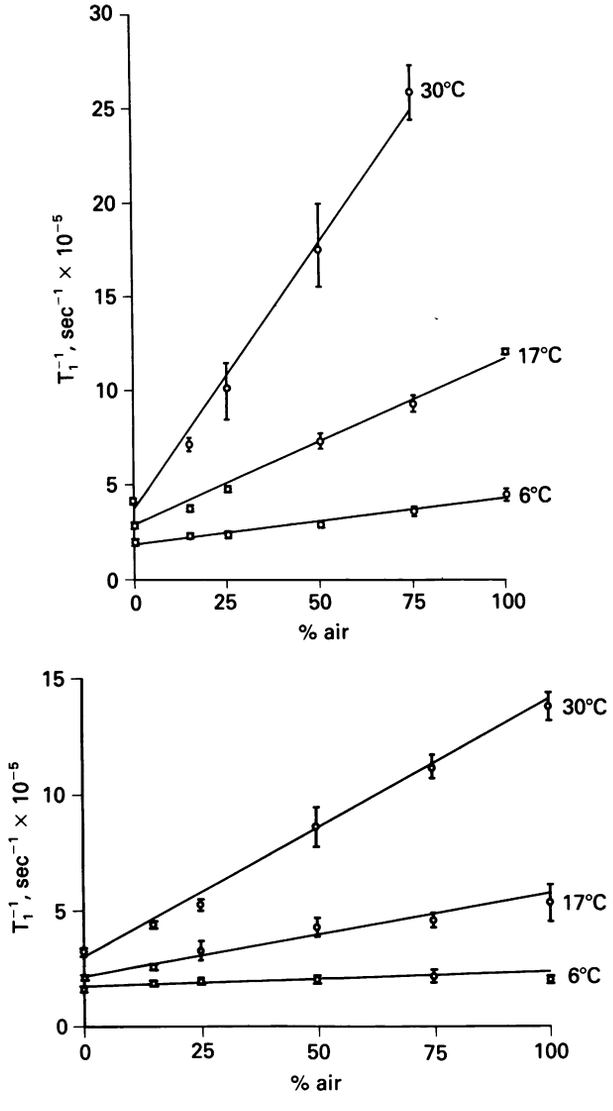

FIG. 5. T_1^{-1} vs. concentration of air at three temperatures: above the phase transition temperature, between the main and pretransition temperatures, and below the pretransition temperature. $Myr_2PtdCho$/spin label ratio, 100:1. (*Upper*) ASL; (*Lower*) CSL.

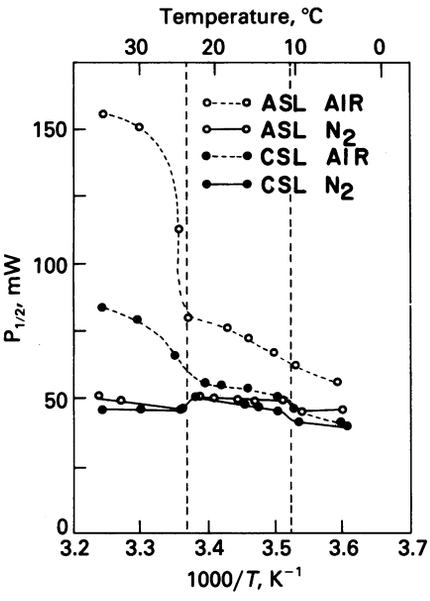

FIG. 6. $P_{1/2}$ data equilibrated with 50% air (broken lines) or nitrogen (solid lines) as a function of reciprocal temperature for CSL (●) and ASL (○).

probability of spin labels in membranes in the absence of air. In the presence of air the factor may be less than 3, depending on the ratio of the bimolecular collision rate with oxygen to the nitrogen nuclear relaxation probability. The range of variation of oxygen-mediated $P_{1/2}$ is much less than for T_1 (Fig. 4) because the intrinsic T_2 tends to have an opposite temperature dependence from that of the bimolecular collision rate between oxygen and spin labels.

An oxygen transport parameter can be defined as

$$W = T_1^{-1}(\text{air}) - T_1^{-1}(N_2) \propto D_o[O_2].$$

This parameter is obtained by subtracting the data of Fig. 4 *Left* from those of Fig. 4 *Middle*; the results are shown in Fig. 4 *Right*. Extrapolation has been made from 50% to 100% air. The overall variation of the oxygen transport parameter with respect to temperature (0°C to 36°C) can be as large as a factor of 100.

Translational diffusion of oxygen in a membrane is presumably described by an axially symmetric tensor with the principal axis coinciding with the normal to the bilayer and with the magnitudes of the elements of the tensor dependent on the distance from the surface. The exchange integral is thought to be greater for an approach of oxygen to the spin label that occurs along the p_z orbital than for approaches along x or y (23). In addition, y collisions are less effective because the nitroxide radical is protected by methyl groups on which the spin density is very low. Referring to the molecular structures of Fig. 1, one might expect the stearic acid labels to be more sensitive to diffusion of oxygen parallel to the normal to the bilayer, which we call vertical diffusion, whereas the sterol-type labels would be more sensitive to diffusion parallel to the surface of the bilayer.

This model of anisotropic diffusion is used to interpret the data of Fig. 4 *Right*. Above the main phase transition, the ratios W(CSL)/W(5-SASL) and W(ASL)/W(16-SASL) are close to unity, indicating that the diffusion tensor tends to be isotropic. W(ASL) ≈ W(16-SASL) > W(CSL) ≈ W(5-SASL), indicating a higher bimolecular collision rate in the center of the bilayer, presumably caused both by higher concentration and more rapid diffusion. Below the pretransition, W(CSL) ≪ W(5-SASL), indicating facile vertical diffusion near the surface. At lowest temperature, W(ASL) ≪ W(16-SASL), suggesting facile oxygen transport across the entire membrane. The region between phase transitions is complex in behavior, and it does not seem appropriate to suggest an interpretation. It is noted that the phase transitions apparently cause abrupt changes in vertical diffusion, as indicated by W(5-SASL) and W(16-SASL) data in Fig. 4 *Right*, but gradual change in horizontal diffusion, as indicated by W(CSL) and W(ASL).

The transport parameter W, an experimental observable for small molecule transport, can be related to physiological phenomena such as chemoreception (24) and passive or facilitated transport.

This work was supported by Grants GM-27665, GM-22923, and RR-01008 from the National Institutes of Health.

1. Berliner, L. J., ed. (1979) *Spin Labeling, Theory and Applications* (Academic, New York), Vol. 2.
2. Hyde, J. S. & Thomas, D. D. (1980) *Annu. Rev. Phys. Chem.* **31**, 293–317.
3. Popp, C. A. & Hyde, J. S. (1981) *J. Magn. Reson.* **43**, 249–258.
4. Subczynski, W. K. & Hyde, J. S. (1981) *Biochim. Biophys. Acta* **643**, 283–291.
5. Huisjen, M. & Hyde, J. S. (1974) *Rev. Sci. Instrum.* **45**, 669–675.
6. Forrer, J. E., Wubben, R. C. & Hyde, J. S. (1980) *Bull. Magn. Reson.* **2**, 441.
7. Fischkoff, S. & Vanderkooi, J. M. (1975) *J. Gen. Physiol.* **65**, 663–676.
8. McDonald, G. G., Vanderkooi, J. M. & Oberholtzer, J. C. (1979) *Arch. Biochem. Biophys.* **196**, 281–283.
9. Windrem, D. A. & Plachy, W. Z. (1980) *Biochim. Biophys. Acta* **600**, 655–665.
10. Hyde, J. S. (1979) in *Time Domain Electron Spin Resonance*, eds. Kevan, L. & Schwartz, R. N. (Wiley, New York), pp. 1–30.
11. Percival, P. W. & Hyde, J. S. (1975) *Rev. Sci. Instrum.* **46**, 1522–1529.
12. Freed, J. H. (1974) *J. Phys. Chem.* **78**, 1155–1167.
13. Freed, J. H. (1979) in *Time Domain Electron Spin Resonance*, eds. Kevan, L. & Schwartz, R. N. (Wiley, New York), pp. 31–66.
14. Gaffney, B. J. & McConnell, H. M. (1974) *J. Magn. Reson.* **16**, 1–28.
15. McConnell, H. M. (1976) in *Spin Labeling, Theory and Applications*, ed. Berliner, L. J. (Academic, New York), pp. 525–560.
16. Hemminga, M. A. (1975) *Chem. Phys. Lipids* **14**, 151–173.
17. Schindler, H. & Seelig, J. (1974) *J. Chem. Phys.* **61**, 2946–2949.
18. Müller-Landau, F. & Cadenhead, D. A. (1979) *Chem. Phys. Lipids* **25**, 299–314.
19. Sanson, A., Ptak, M., Rigaud, J. L. & Gary-Bobo, C. M. (1976) *Chem. Phys. Lipids* **17**, 435–444.
20. Träuble, H. & Eibl, H. (1974) *Proc. Natl. Acad. Sci. USA* **71**, 214–219.
21. Papahadjopoulos, D. (1968) *Biochim. Biophys. Acta* **163**, 240–254.
22. Berliner, L. J. (1978) *Methods Enzymol.* **49**, 466–470.
23. Molin, Y. N., Salikhov, K. M. & Zamaraev, K. I. (1980) *Spin Exchange* (Springer, New York), pp. 19–20.
24. Adam, G. & Delbrück, M. (1968) in *Structural Chemistry in Molecular Biology*, eds. Davidson, N. & Rich, A. (Freeman, San Francisco), pp. 198–215.